scientific reports

Check for updates

OPEN

Combining response surface methodology and measurement system analysis to identify melt flow index of hygrothermal-sensitive composites

Ning Su[1], Xiaoling Liu[2], Xiang Chen[1], Jiafei Gu[3] & Jing Bai[4]✉

The key aspects of this work were the enhancement of the repeatability of the melt flow index (MFI) measurement and improvement of reproducibility for testing certain hygrothermal-sensitive materials, which are sensitive to temperature and water content. The present work was structured into two main parts. Firstly, several test variables affecting MFI were evaluated using a blocked response surface methodology (RSM), and multivariable linear regression was applied to assess the influence of test load, test temperature, drying time, and pre-heat time on MFI of nylon-based thermoplastic. The impact of test variables was analyzed by 20 randomized experiments, including 8 "two-level full factorial run" with 6 "centre run" replicates. The test parameters were optimized based on the RSM result and the ANSYS® simulation-based prediction. Later, these process variables were chosen to evaluate repeatability and reproducibility of the test of PA and 20 wt% vCF/PA for verification, which was diagnosed by measurement system analysis (MSA) for consistency and reliability assessment. The optimization test parameters for these composites were pre-heat time 1–3 min and drying time 6.6 h. By this means, the repeatability and reproducibility of these composites were up to 3.179% and 12.208%, respectively. The findings provide a practical testing framework that reduces uncertainty, enhances credibility, and ensures meaningful use of MFI in process optimization and quality control for polymer composite manufacturing.

Keywords Melt flow index (MFI), Measurement system analysis (MSA), Response surface methodology (RSM), Temperature-sensitive, Moisture-sensitive, Hygrothermal-sensitive

Melt flow index (MFI) is generally considered a crucial rheological property of composites, which is a simple, easily obtainable viscosity parameter from a relatively inexpensive apparatus within the technical and financial means of thermoplastics processors[1]. It is widely accepted as the direct measurement for processability and correlates with final product properties[2]. Notably, the difference threshold value of MFI is required depending on the various processing methods, as shown in Table 1. For example, the MFI value of conditionally recommended thermoplastics for injection molding is 0.43 to 44.5 g/10min[3]; for coating, approximately 20 g/10min, and for extrusion, the optimized value is about 1.5 to 22 g/10min[4]. Moreover, during the fabrication of high-density polyethylene (HDPE) and isotactic polypropylene (PP), the MFI value should be even lower (ranging from 0.3 to 0.5 g/10min) due to the lower intermolecular cohesion and low inherent fibrillation tendency of the polymer[1]. Meanwhile, the 3D printing technology based on extrusion and fusion of a thermoplastic filament, which is known as Fused Deposition Modeling (FDM), is more reliable on reasonable MFI of the printing feedstock materials. Tian et al.[5] analyzed the influence of MFI on flexural strength and modulus of 3D printed carbon fiber reinforced PLA composites, and wang et al.[2] reported different properties of seven commercial PLA feedstocks, finding the threshold value of MFI (~ 10 g/10 min) for successful printing. A range of studies[6–11] have investigated the effect of metal powder as reinforcement in a polymer matrix on mechanical properties. The evaluation of MFI determined the optimized compounding ratio of filler materials. However, the MFI result

[1]College of Digital Technology and Engineering, Ningbo University of Finance and Economics, Ningbo 315175, China. [2]Faculty of Science and Engineering, University of Nottingham, Ningbo 315199, China. [3]School of Intelligent Manufacturing, Hangzhou Polytechnic, Hangzhou 311402, China. [4]Nottingham University Business School China, University of Nottingham, Ningbo 315199, China. ✉email: jing.bai@nottingham.edu.cn

Forming method	Typical application/methods	MFI (g/10min)	Total MFI range (g/10min)
Injection molding	Toys, household articles, Screw caps	3–13	0.43–44.5[3,21]
	Beer cases	13–25	
	Mass production of household articles, non-deposit goods	25	
	High-speed injection	30-44.5	
Extrusion	Blocks	0.05–0.15	0.05-13[4,21]
	Pipes, round bars	0.1–1.3	
	Films/ Blown film extrusion	0.1–0.4	
	Fuel oil tanks/Blow molding	0.4–0.7	
	Hollow bodies/Blow molding	1.3-3	
	Toys, household articles, Screw caps/Blow molding	3–13	
Compression molding	Profile, blocks	0.05–0.15	0.05-2[4]
	Pipes	1–2	
All method	High-density polyethylene (HDPE) and isotactic polypropylene (PP)		0.3–0.5[1]
Film, monofilament	Thermoplastics		5–15[4]
Coating	Thermoplastics		< 20[4]
3D printing	Composites, PLA		2.411-10[2,22]

Table 1. MFI of typical thermoplastics for various end uses or processing methods.

is questionable and relatively difficult to operationalize when applying the composites fabrication process[12]. The main reason for this unsatisfactory situation is the lack of perceived credibility of MFI, which necessarily leads to relationships with the equivalent corresponding process parameters. Although many researchers characterize the dependence of the rheological behaviour and efficiency on the processing conditions as a good indicator of process optimization for composites, it has not been considered a fundamental polymer property[1]. On the one hand, thermal degradation, cross-linking, or further polymerization influences the forming and mechanical properties of the end products, resulting in a higher MFI[1]. An additional reason is that the temperature and shear rate (extrusion load/pressure) encountered in an actual polymeric composites processing differ significantly from those employed in the MFI test. Meanwhile, only under the intermediate shear rate, ranging from 0.1 /s to 104 /s, the result of MFI measurement plays an appropriately and credibly instructive role in the fabrication due to the insensitivity of MFI to the effects of molecular-weight distribution[13]. Normally, the variation in molecular weight distribution had a minor influence on flow behavior at the intermediate shear rate, whereas the corresponding MFI shows a meaningful interpretation of polymer flow[14]. Alternatively, the moisture content of the tested materials would cause the tendency of the speed degradation rate of a polymer as a result of relatively poor repeatability and reproducibility of MFI, especially for those with a hygroscopic property that are also sensitive to water, such as PET, PBT, and PA[15]. Despite all these limitations, MFI remains an important quality control rheological parameter during composite fabrication[16]. The key success of obtaining a reliable MFI value is tightly controlling the pre-heating time, extrusion time, and drying time and consistent between test instrument and the effect on uncertainties of the test, however, few studies have analysed these test variables[12,15,17] and no research, according to author's best knowledge, focus on the impact of processing parameters on related to the test load of MFI.

Moreover, although the International Organization for Standardization has published ISO 1133-2:2011(E) standard, especially for testing materials sensitive to time-temperature history or moisture, the test procedures are expensive or difficult to implement. Besides, the precision of the method is not known because interlaboratory data are not available, whilst the material form (e.g., pellets or flakes), fabrication parameters (e.g., grind force or pressure), and filler content, which significantly affect the accuracy of the test, are not thoroughly investigated[12,15]. The six research gaps of the current test standard for hygrothermal-sensitive materials are as follows, as shown in Fig. 1:

Q1-Difficulty of tester criteria check The temperature distribution of the MFI tester needs to be verified before the measurement. However, the temperature measuring device is challenging to locate and manipulate precisely. In the majority of cases, it cannot even be implemented.

Q2-Unknown test error the materials (i.e., powders, flakes, and large pellets) must be formed into compacted charges to obtain repeatable results (by reducing issues associated with air entrapment and voids). However, the performance is harsh and easily causes thermal degradation/history, introducing an unknown error that affects the accuracy of the test result[18].

Q3-Over-drying for pre-conditioning The standard does not detail the drying time of these materials. The over-drying before the testing would cause a dramatic decrease in MFI[12].

Q4-Expensive of water content test the water content test is expensive and challenging to implement.

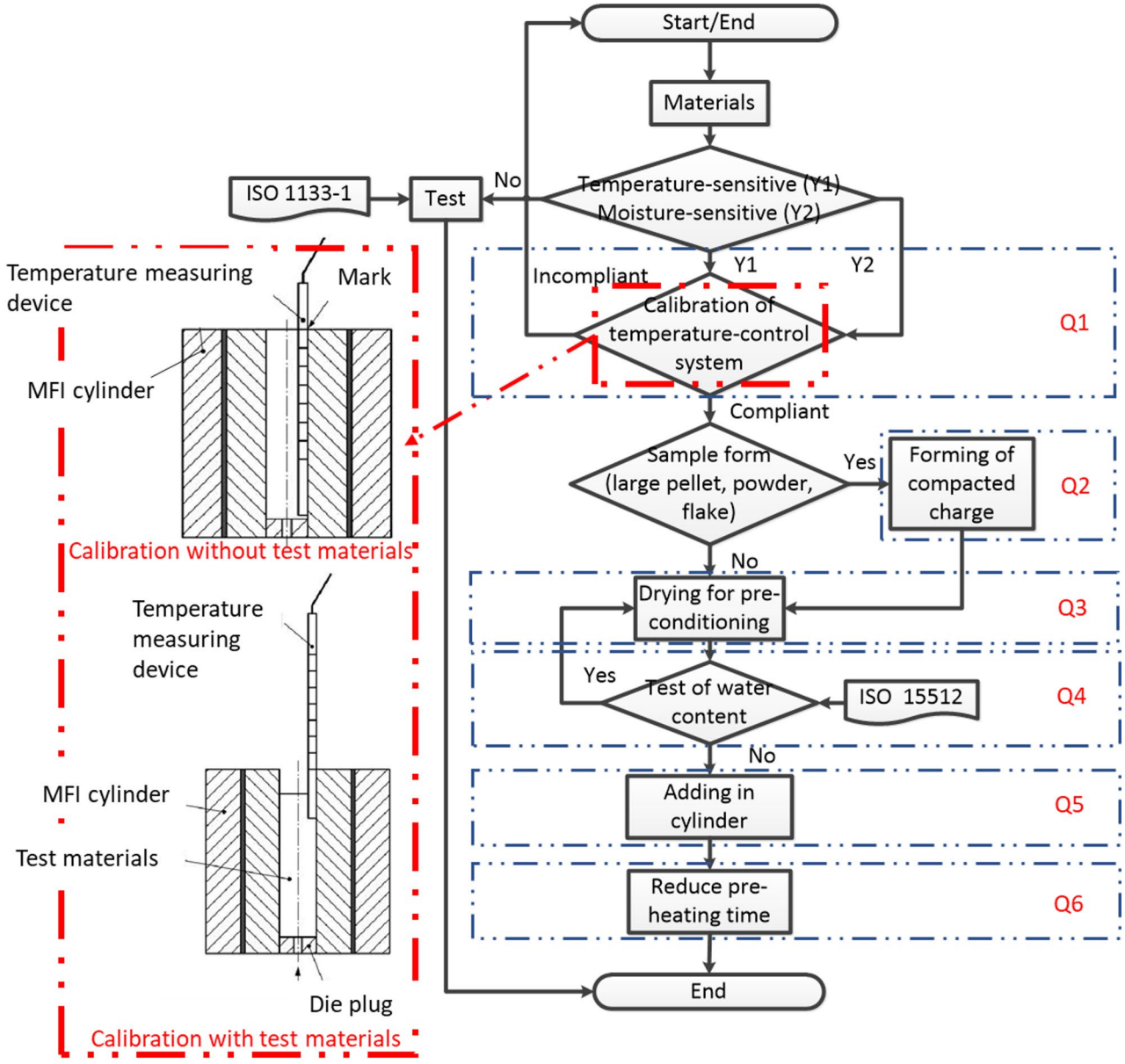

Fig. 1. MFI test procedures of ISO 1133-2 and relevant acknowledged gaps (□: Step of flow chart; ◇ Decision; ▭: Supplementary test standard).

Q5-Impossible adding within a short time To prevent moisture during the test, the complete adding process of materials within 0.5–1 min, which is impossible to accomplish due to the semi-molten materials clogging at the entrance of the tester, as shown in Fig. 2b.

Q6-Unknown pre-heating time A shorter pre-heating time is required to prevent thermal degradation. However, the time has not been pointed out for specific cases.

In this paper, the MFI test variables, which were set up under conditions closely associated with actual fabrication processing (3D printing processing), were investigated by measurement system analysis (MSA) and response surface methodology (RSM) for the determination of repeatability and reproducibility of the test, thereby decreasing the overall uncertainty of the experiment and optimizing apt test variations, as shown in Fig. 3.

Figure 3 presents an integrated methodological framework that systematically resolves the Q1–Q6 bottlenecks identified in Fig. 1. Traditional ISO 1133-2 procedures for hygrothermal-sensitive materials often suffer from calibration difficulty, undefined pre-conditioning parameters, and poor reproducibility. This study combines RSM and MSA in a sequential, feedback-controlled workflow to overcome these issues.

Firstly (**RSM optimization stage**), key variables were statistically modeled using blocked factorial and central-composite designs, particularly drying and pre-heating duration. This quantitative approach replaced

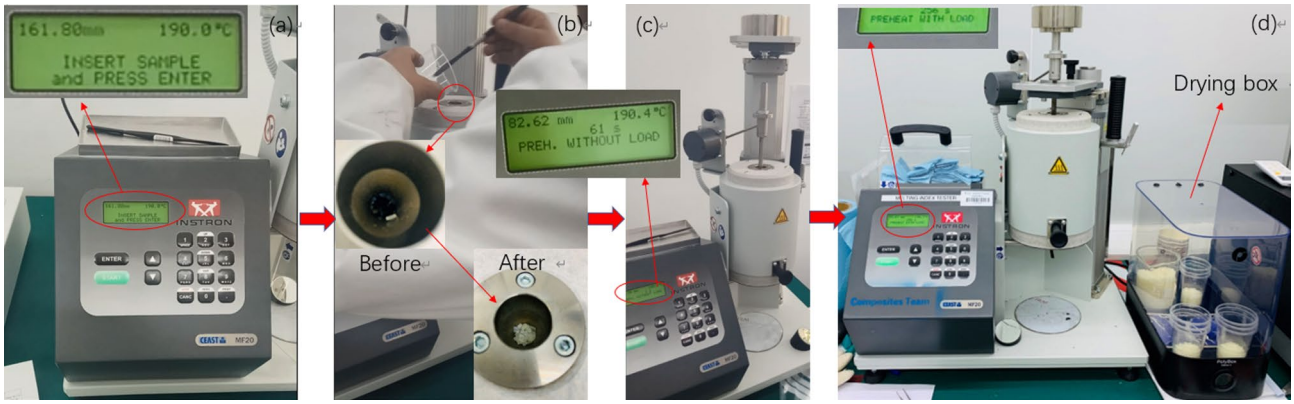

Fig. 2. MFI test procedure (**a**). Target temperature stabilized; (**b**). Materials adding; (**c**). Pre-heat without load; (**d**). Extrusion with load.

empirical parameter selection and costly trial-and-error testing, identifying optimal conditions to resolve **Q3**, **Q4**, and **Q6**.

Secondly, **simulation validation** was conducted to verify the pre-heating time of pure PA obtained from the result of RSM-based statistical analysis in the previous stage. Sequentially, the optimized pre-heating time for vCF/PA was predicted through computational modeling using transient heat-conduction analysis via ANSYS, eliminating the uncertainties related to unknown heating stabilization (**Q6**).

In the **MSA verification stage**, measurement bias and linearity were evaluated to replace traditional thermometer-based calibration (**Q1**). PE was selected as a benchmark due to its stability and wide load range[12], while PA and vCF/PA were used to assess applied precision. Randomization of specimen forms (pellets, flakes, powders) minimized systematic errors and mitigated thermal-history effects[19]. Randomizing shapes is a common strategy in experimental design to eliminate systematic errors and ensure that the experimental results are objective, unbiased, and reproducible[20]. To a certain extent, this approach serves as a practical solution to **Q2**.

Since **Q2** and **Q5** were practically unsolvable under the existing testing framework, this study adopted a result-evaluation approach. Under the conditions that best conform to ISO 1133-2:2011(E) requirements, the experimental outcomes were directly assessed using the intuitive scale: Number of Distinct Categories (NDC) index. When the calculated value satisfied NDC ≥ 5, the measurement was considered fully valid and acceptable, indicating a reliable and reproducible testing system.

Combining RSM and MSA, Q1-Q6 outlined in Fig. 1 were addressed: calibration uncertainty was replaced by quantitative validation, moisture and pre-heating effects were optimized statistically and simulated, and measurement consistency was verified statistically.

Materials and methods

Materials

In this study, the polyethylene (PE) has been used as the reference for benchmarking, while the 3D printing feedstock filaments, the neat polyamide (PA), and 20 wt% virgin carbon fiber reinforced polyamide (vCF/PA) were tested for assessing repeatability and reproducibility using several statistical methods. Details of these materials are given in Table 2.

Melt flow index (MFI)

MFI provides an assessment of the average molecular mass of the material; thus, the inverse measurement of the melt viscosity is estimated following a four-step procedure (a, b, c, and d) as shown in Fig. 2 (details in Appendix A)[24]. The MFI of tested materials was investigated using an MF20 CEAST (Instron, Norwood, MA, USA) following the ISO 1133-2:2011(E) standard. Due to the hygroscopy of the polymer and composites, all the specimens were kept in a drying oven for specific hours at 103 ± 2 °C before the test for pre-conditioning and then were kept in drying box (PolyBox™ Edition II, Polymaker®, Shanghai, China) at a temperature of 20 ± 2 °C and humidity of 12 ± 3% R.H during the test as shown in Fig. 2d.

Experimental design

For conducting this study, the design of the experiment (DoE) and the validation of the results were performed using Minitab® v17.2.1 software. The DoE of testing of pure PA was based on a blocked response surface methodology (blocked RSM). This study focuses on the impact of moisture content and thermal degradation on the MFI test, so the drying time (pre-conditioning), pre-heating time (procedure Fig. 1c), and test temperature were controlled factors. Notably, the temperature was input in reciprocal form: 1/T. According to the Arrhenius-Eyring formula, molecular motion and flow behavior are governed by thermally activated processes, where the probability of overcoming an energy barrier follows the Boltzmann distribution and depends exponentially on the reciprocal form of temperature, as described by the Arrhenius and transition state theories[25–27] (for details, see calculation of Appendix B). Meanwhile, to achieve a meaningful statistical difference with minimum trial runs, the test loads of MFI were chosen as 2.16 and 5 kg as RSM blocks[12,19,28–33] (details are in Appendix C).

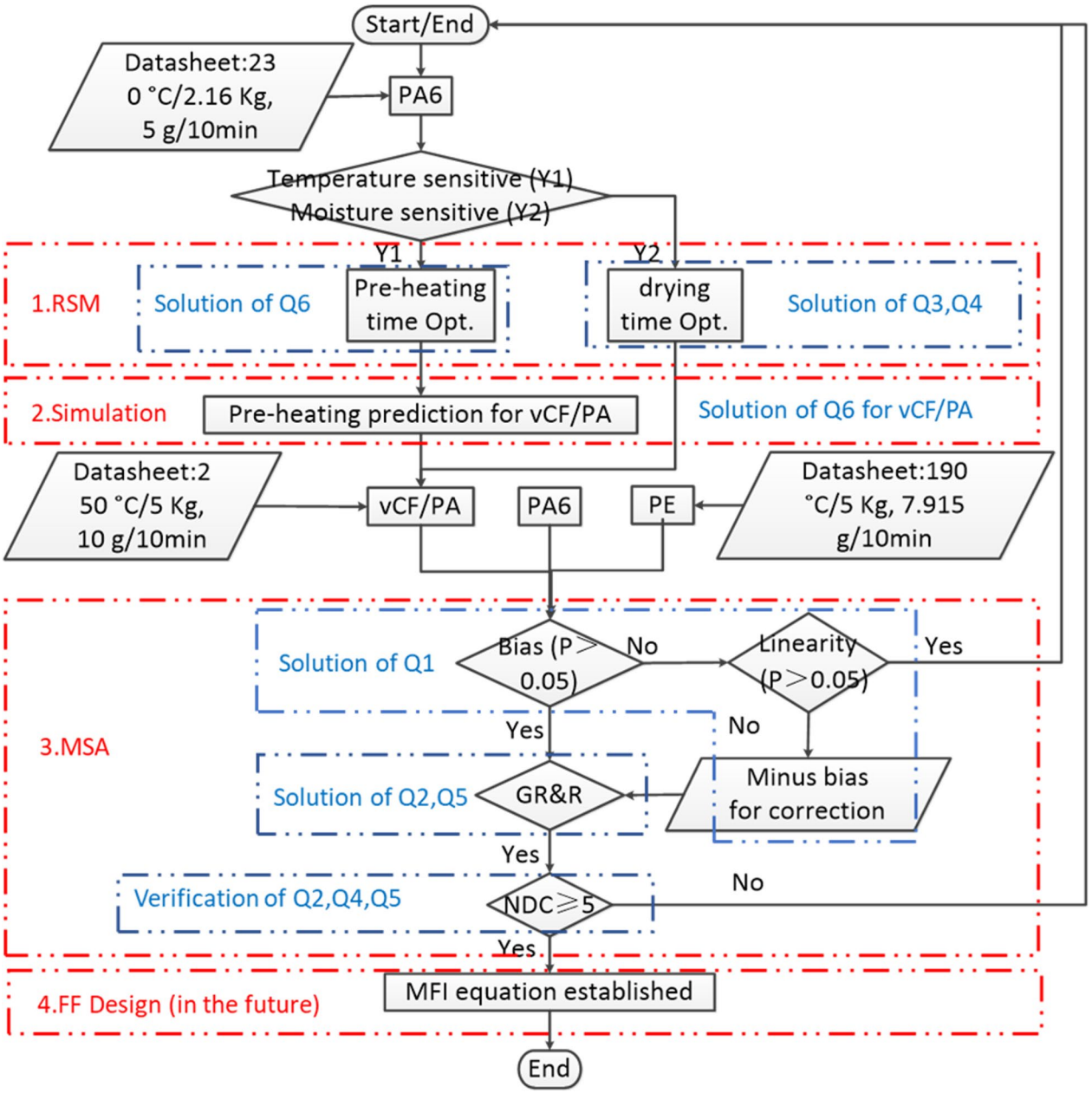

Fig. 3. Novel MFI test combining RSM & MSA (□: Step of flow chart; ◇: Decision; ▱: Data).

Material	Grade	Brand	Test condition	Reference MFI (g/10min)
PE	0801.778	Instron *	190 °C /2.16 kg	7.915 ± 0.516
PA[23]	ePA_nature	Esun *	230 °C /2.16 kg	~ 5.000
vCF/PA[23]	20 wt% fiber-filled PA	Esun *	250 °C /5kg	~ 10.000

Table 2. Datasheet of tested materials.

Totally, 20 experiments, including 8 "two-level full factorial run", 6 "star points run", and 6 "center runs" were performed as shown in Table 3. The maximum and minimum values of the full factorial runs and star points runs were coded as ± 1 and $\pm\alpha$, respectively, while the centre runs were coded as 0. Alternatively, the centre runs consisted of two parts, four centre runs from block 5 kg and two center runs from block 2.16 kg.

After the RSM experiments, the calibration and verification of the tests were performed by measurement system analysis (MSA). The measurements of PE, PA, and vCF/PA using optimized test parameters by RSM were analyzed by trial tests at three different times of the day (9:00 a.m., 2:00 p.m., and 5:00 p.m.) following the ISO

Blocks	1	2		Coded levels			$\alpha = 1.633$	
Test loads (kg)	5	2.16	Factors	-1	0	1	$-\alpha$	$+\alpha$
			A: 1/Temperature (°C)	1/250	1/230	1/210	1/260	1/200
			B: Pre-heat time (min)	2	3	4	1	5
			C: Drying time (h)	3	8	12	0	15

Table 3. Variables in RSM experimental design for PA.

Materials	Test time	Test temperature (°C)	Test load (kg)	Pre-heat time (min)	Drying Time (h)
PE	9:00 a.m./ 2:00 p.m./ 5:00 p.m.	190	2.16	5	0
PA	9:00 a.m./ 2:00 p.m./ 5:00 p.m.	230	2.16	3	6.6
vCF/PA	9:00 a.m./ 2:00 p.m./ 5:00 p.m.	250	5	1	6.6

Table 4. Nested design of a G experiment.

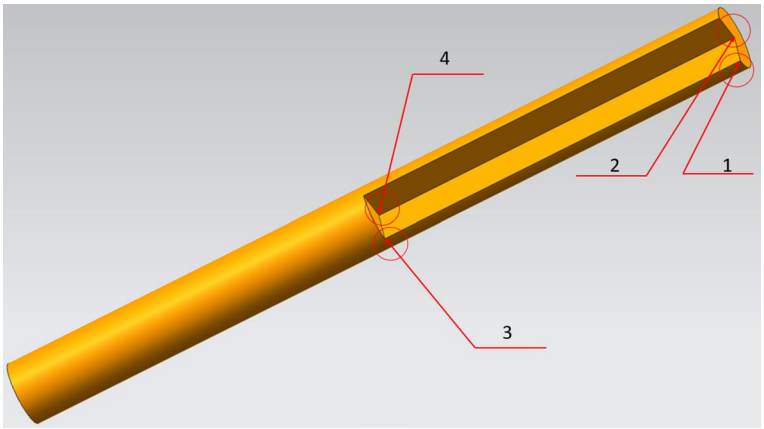

Fig. 4. Thermal model of tested materials.

5725-2:2019(E)[15] and determined via %GageR&R (abbr. G experiment) capability evaluation[34]. Also, because of the destructive nature of the tests, the experiments were conducted using nested analysis[35] (as shown in Table 4). Notably, the pre-heat time of PA and vCF/PA was conducted according to the simulation-based prediction described in the later result section. The varying shapes of PA and vCF/PA were used randomly in these tests to remove the influence of thermal history on MFI.

Transient analysis for thermal conductivity

The optimized pre-heat time via RSM was verified by ANSYS Inc v15.0® software. According to the internal dimensions of the MFI tester, the tested materials were simplified into a $\varnothing 9.550 \times 115$ mm homogeneous cylinder, as shown in Fig. 4. Four reference points were selected: when the temperature of Point No. 4 achieved the setting temperature, the stabilization time is the pre-heat time. The analysis was conducted using the solver of the transient thermal conductivity problem. The simulation of the pre-heat time of pure PA was the verification of the RSM result, while the pre-heat time calculation of 20 wt% vCF/PA was used as a forecast of the nested G experiment. The pre-heat time of the two materials was determined under the conditions of 200 °C, 230 °C, and 250 °C to investigate the effect of temperature on stabilization time.

Results and discussion

Evaluation of the influence of test parameters

The results of MFI at the different test conditions are summarized in Table 5 (full details are in Appendix E). The experiments were randomized to prevent the influences of unknown nuisance variables from contaminating the results[36]. It can be seen that poor repeatability (statistical outlier>6%[12]) occurred without sufficient drying time, such as Run 5, 12, 14, especially, without PA drying, the repeatability value up to 41.128% which is highly abnormal. Vice versa, such as Run 18, over-drying of the PA before the testing would cause a dramatic decrease of MFI (3.535 < 5 g/10min) due to the further polymerization when drying[12]. The plots of the residuals versus fitted value are shown in Fig. 5, which verifies the assumption that the difference between the observed values (actual experimental values) and the computed values (model predicted values) are randomly distributed and

Run Order	Std Order	Blocks Load (kg)	1/T (1/ °C)	Pre-heat time (min)	Drying time (h)	MFI (g/10min)			Note
						Mean	SD	Repeatability limit (2.8×S_r %)	
2	6	5	1/210	2	12	4.545	0.003	0.185	FF
5	2	5	1/210	2	3	6.042	0.235	10.890	FF
7	10	5	1/230	3	8	13.349	0.028	0.587	C
12	4	5	1/210	4	3	6.469	0.216	9.349	FF
14	17	2.16	1/230	3	0	6.092	0.896	41.182	S
18	18	2.16	1/230	3	15	3.535	0.007	0.554	S
20	20	2.16	1/230	3	8	5.256	0.028	1.492	C

Table 5. Summary of experimental data obtained from the RSM runs. FF: full factorial runs; C: center runs; S: star point runs.

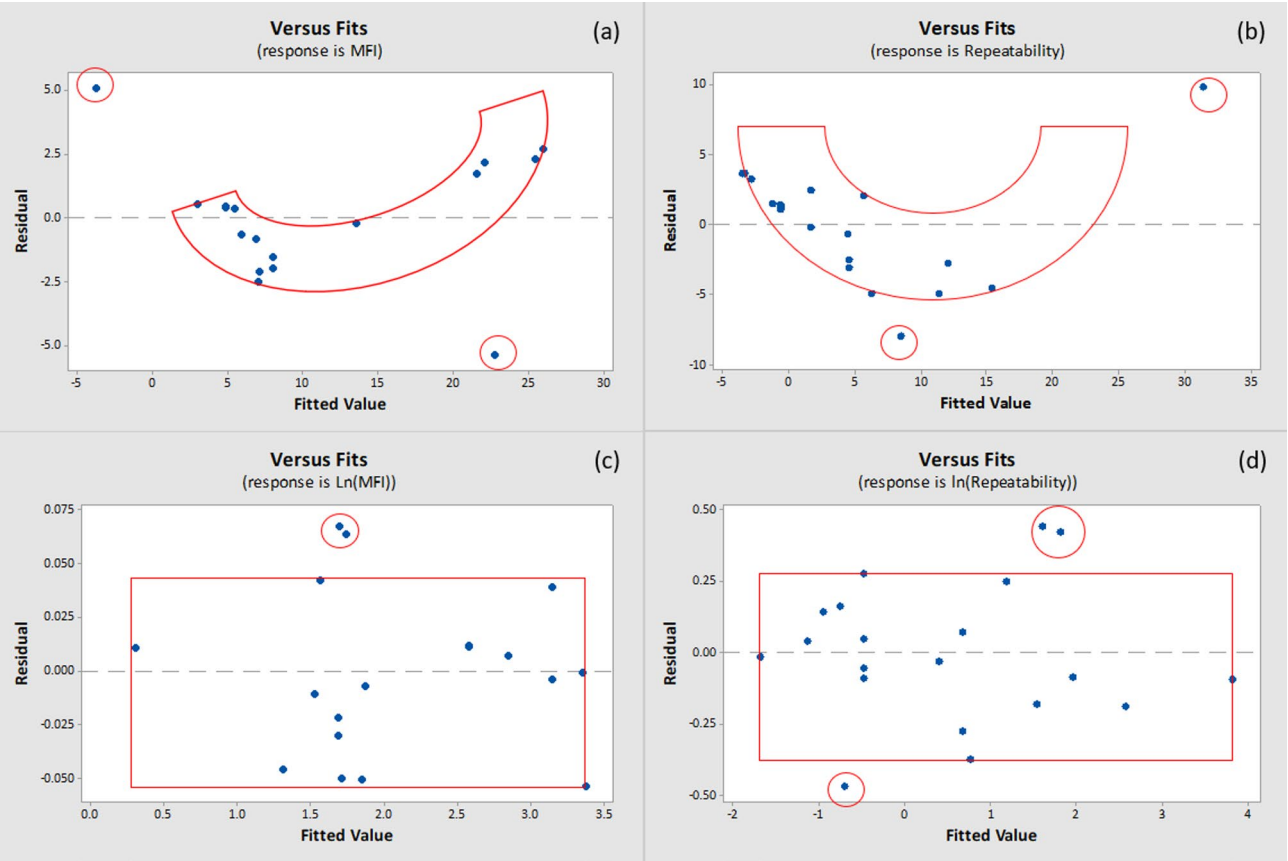

Fig. 5. Residual versus fitted value for (**a**). MFI (**b**). Repeatability (**c**). Ln (MFI) (**d**). Ln (Repeatability) Note: ○ Unusual Observations ∪ Curvature distribution □ Uniform distribution.

have constant variance[37], therefore, indicating the quality of the fitting. When MFI and correlated repeatability (2.8×Sr %) were defined as responses, as shown in Fig. 5a and b, the curvilinear pattern illustrated the contradiction of the assumption. Meanwhile, some of the points were a serious departure from equilibrium. Despite the deviation from the fitted value, most of the residuals fell randomly on both sides of 0 with uniform distribution, if the logarithm of the responses was chosen. It can be generally concluded that the residuals for both logarithms of MFI and correlated repeatability as responses led to no considerable scattering residuals, as shown in Fig. 5c and d, which was consistent with the variant Arrhenius-Eyring formula (Eq. B3, Appendix B). Further, analysis of variance (ANOVA) for this blocked design was conducted to find the significant controlled factors affecting the MFI using the probability value (P-value) estimation, which is defined as a significance level leading to the rejection of the null hypothesis ($P < \alpha = 0.05$) [19,36,38,39] (details are in Appendix D). The relative significance of the three independent variables and their interaction with blocks is shown in Fig. 6 using the corresponding Fisher's variance ratio ($F_{1-\alpha} = 5.12$) where the black line denotes the onset of significant effects. It is evident from these plots that temperature, drying time, and test load have a significant

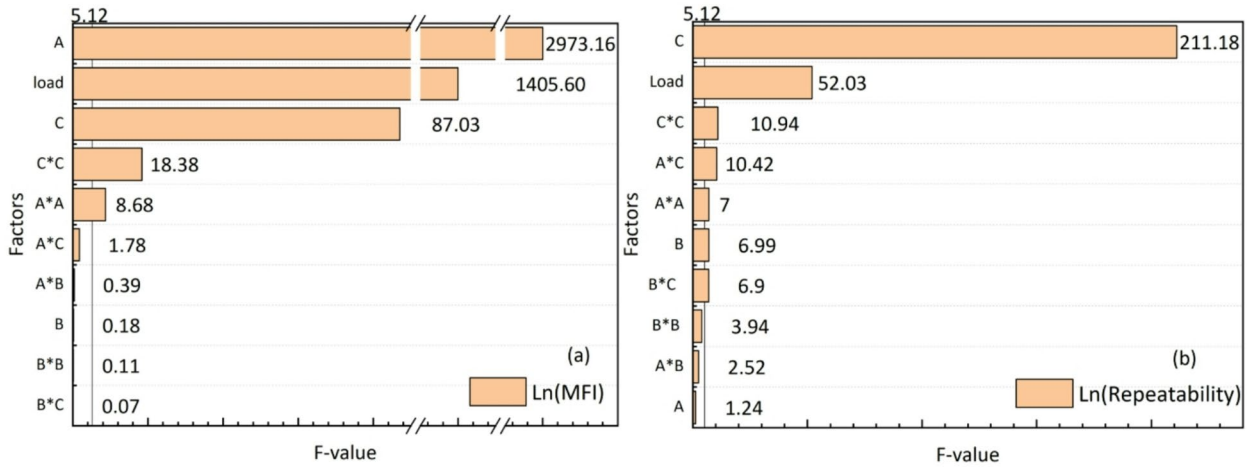

Fig. 6. Pareto chart of F-value (**a**) F-value of Ln (MFI) (**b**) F-value of Ln (Repeatability). Note: A 1/T, B Pre-heat time, C Drying time.

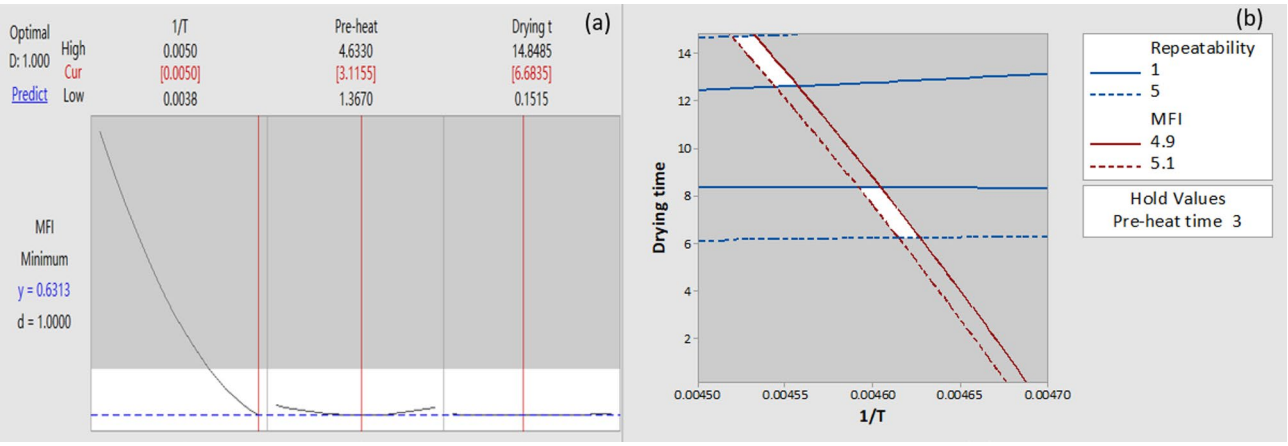

Fig. 7. Experimental optimization of PA (**a**) Plot of steepest ascent search approach (**b**) Plot of overlaid contour.

impact on both MFI and corresponding repeatability. While pre-heat time only influenced the repeatability of the experiment due to the thermal degradation[19], similarly, some interactions did have impacts on MFI and repeatability to a certain extent, but were less pronounced than first-order independent variables. From the RSM data, it would make a prediction based on the steepest ascent search methodology and overlaid contour plot calculation[36,40], the white region of the operating window illustrated the constrained conditions for optimization as shown in Fig. 7. Figure 7a depicts the optimized test parameters during the MFI measurement of pure PA, they are, respectively, temperature 200 °C, pre-heat time 3 min and drying time 6 h and 40 min. As a result, when the pre-heat time was held at 3 min, considering that the reasonable repeatability of the experiment should be less than 5% [12] and the corresponding MFI value of 5.000 ± 0.089 g/10min, the drying time was in the range from 6 to 8 h or 12–14 h. Plus, the over-heat time would decrease the value of MFI, so the drying time was 6.6 h as shown in Fig. 7b. Later, the test of water content was conducted following ISO 62 standard, after drying of 6.6 h, the weight loss of PA was terminated indicating the total evaporation of the water content of polymer (C_{PA}= 2.63 ± 0.03%).

Analysis of pre-heat time

Figure 8 illustrates the transient thermal behavior and stabilization process of pure polyamide (PA) during the preheating stage of the MFI test. The simulation depicts the temperature evolution from ambient to the preset values (200 °C, 230 °C, and 250 °C) along the radial direction of the specimen. Four monitored points (1–4) were selected from the outermost to the core region to analyze the temperature evolution during the heating process. At the beginning of the preheating process, the outermost surface rapidly exceeded 100 °C, whereas the heat was gradually conducted toward the core region. The temperature became radially uniform after approximately 187.2 s, when the deviation across all monitored positions fell below 3.5%. Considering that the MFI test protocol specifies a 90 s preheating period under load (associated with the extrusion rate), the total time required for

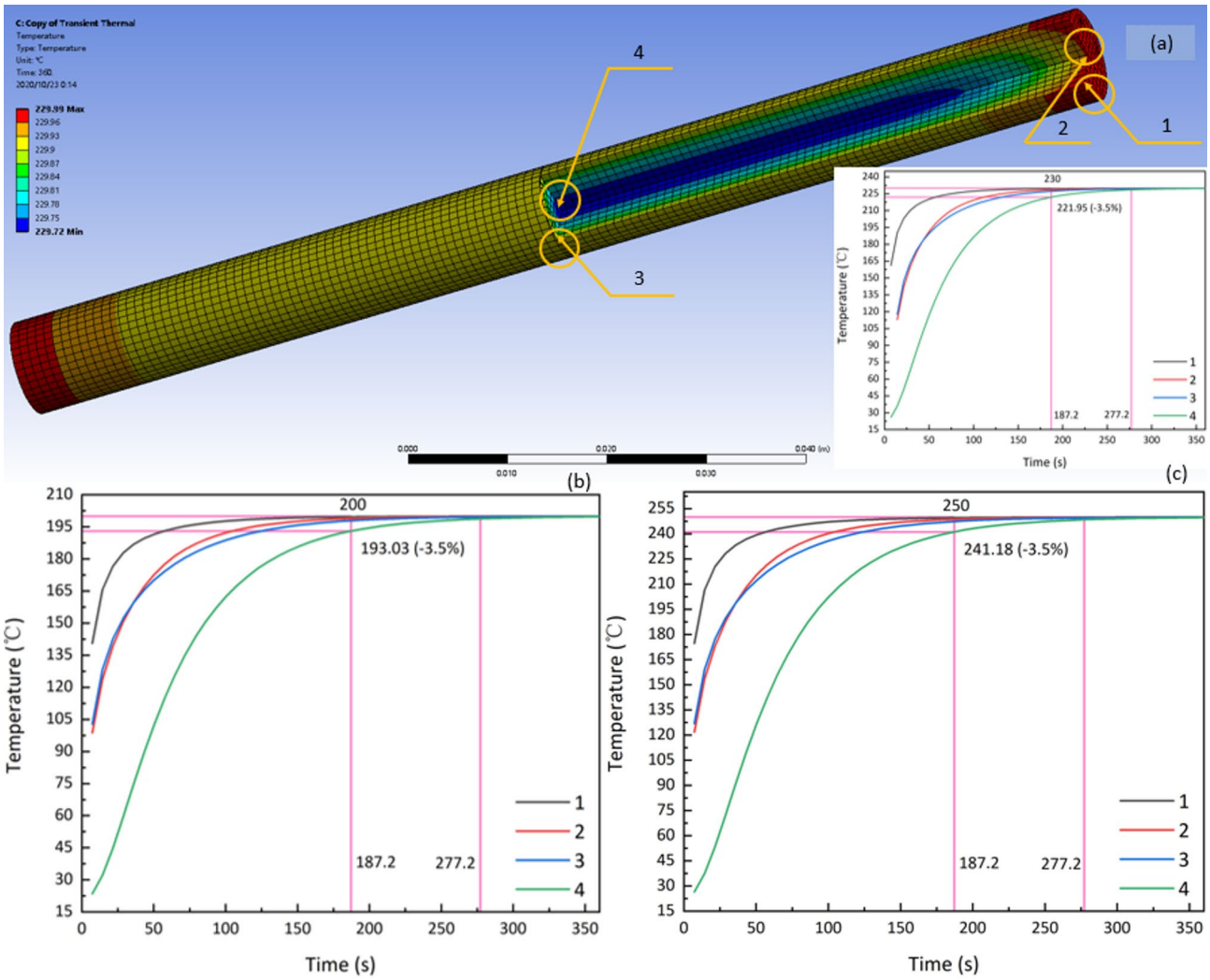

Fig. 8. Thermal simulation of PA (**a**). Temperature distribution and stabilization time of 230 °C (**b**). Stabilization time of 250 °C (**c**). Stabilization time of 200 °C.

complete thermal stabilization was determined to be 277.2 s. Notably, this stabilization duration remained nearly constant across different target temperatures (as shown in Fig. 8a–c), suggesting that the transient response was dominated by the intrinsic one-dimensional heat-conduction characteristics of the PA specimen rather than the magnitude of the external set temperature. The observed temperature-independent behavior can thus be interpreted through the classical 1-D transient heat conduction model as follows:

$$\theta\ (x,\ \tau\ ) = \sum\nolimits_{n=1}^{\infty} A_n \cos\left(\beta_n \frac{x}{\delta}\right) \sum\nolimits_{n=1}^{\infty} \frac{2\sin\beta_n}{\beta_n + \sin\beta_n \cos\beta_n} \cos\left(\beta_n \frac{x}{\delta}\right) \exp(-\beta_n^2 \frac{\alpha\,\tau}{\delta^2}) \quad (1)$$

Where $\theta\ (x,\ \tau\ )$, x and τ represent the dimensionless temperature, distance from the center of the analysis model, and the Fourier number of dimensionless time, the rest are constant coefficients[41]. This indicates that the transient heat conduction behavior is governed by the thermal diffusivity and geometric factors of the tested materials. Therefore, the stabilization time is independent of the initial setting temperature, which aligns with the theoretical prediction of the one-dimensional unsteady heat conduction model. For example, the duration time in Fig. 8b and c is identical, and the duration in Fig. 9a and c is approximately the same. Moreover, according to the prediction of Fig. 7a, the pre-heat time was 186.93s, which was highly consistent with the simulation result. In the same way, the simulation of 20 wt% vCF/PA was used to predict heating time. Due to the excellent thermal conductivity and dissipation of carbon fiber, the stabilization time was even shorter, around 1 min, as shown in Fig. 9. This made it possible to determine the pre-heat time of vCF/PA during the nested G experiment.

Verification via measurement system analysis (MSA)

According to the datasheet of tested materials (as shown in Table 2), three batches were conducted under the recommended test conditions, such as Runs 1, 7, and 13. Each test was measured 8 times, and the maximum and minimum values were excluded for a better confidence level, as shown in Table 6. A hypothesis test was

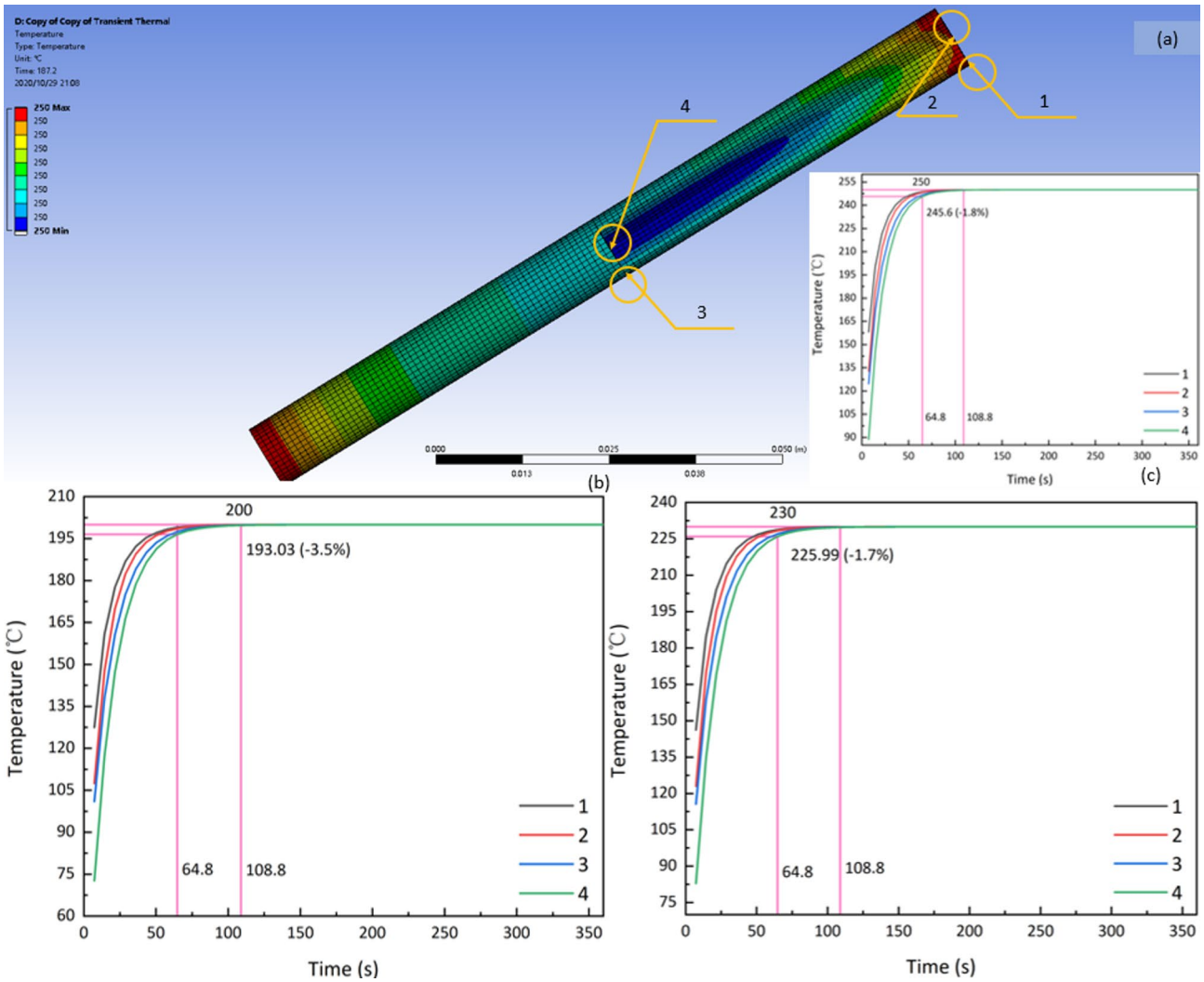

Fig. 9. Thermal simulation of vCF/PA (**a**). Temperature distribution and stabilization time of 250 °C (**b**). Stabilization time of 200 °C (**c**). Stabilization time of 230 °C.

Run order	Materials (g/10min)	Pre-heat Time (min)	Test conditions (°C /kg)	MFI (g/10min)			
				Mean	SD	Repeatability limit (2.8×Sr %)	Reproducibility limit (%)
1	PE (7.915)	5	190 /2.16	7.918	0.016	0.566	0.106
2	PE (7.915)	5	190 /2.16	8.253	0.025	0.848	11.957
7	PA (~ 5)	3	230 /2.16	5.004	0.062	3.469	0.224
8	PA (~ 5)	3	230 /2.16	4.317	0.061	3.956	**38.248**
12	PA (~ 5)	3	230 /2.16	4.424	0.077	**4.873**	32.256
13	vCF/PA (~ 10)	1	250 /5	9.963	0.048	1.349	1.036
17	vCF/PA (~ 10)	1	250 /5	9.777	0.111	**3.179**	6.244
18	vCF/PA (~ 10)	1	250 /5	10.436	0.058	1.556	**12.208**

Table 6. MFI result of MSA.

performed to evaluate bias and linearity. If the P-value is larger than 0.05, the null hypothesis (H_0: bias & linearity existing) was rejected. The horizontal line (Bias = 0) and the average bias of three batches of materials were in the middle of the scope of the confidence interval (CI) of the regression line. All the values were larger than 0.05, which indicated the minimum criterion of the test system was met, as shown in Fig. 10a. This statistically verified that the MFI measurement system is free from systematic error, effectively addressing **Q1** by replacing conventional thermal calibration with a quantitative verification method. The outcome confirmed that the

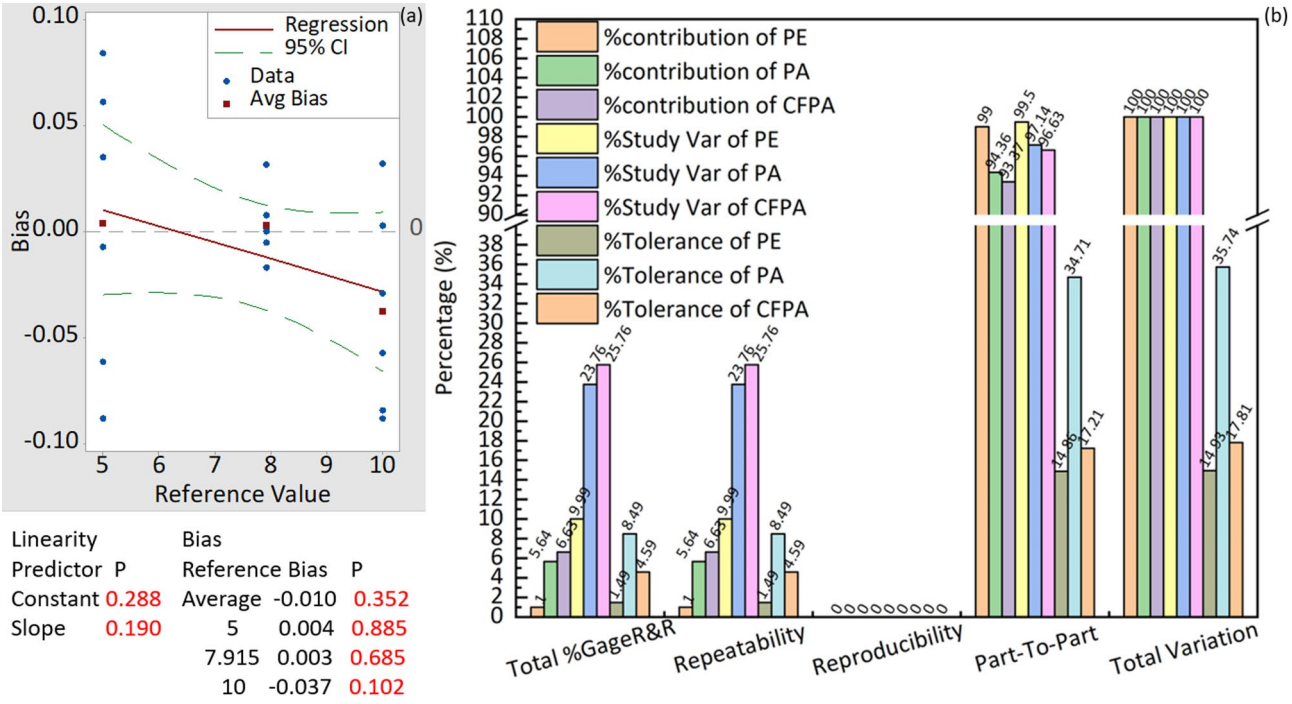

Fig. 10. Plots of MSA (**a**). Linearity and bias of test system (**b**). Repeatability and reproducibility of PE, PA, and vCF/PA.

testing apparatus operates within unbiased limits, thereby ensuring the credibility of subsequent repeatability and reproducibility evaluations.

The evaluation of the measured variation due to the test system and process variation was analyzed by a nested G experiment. The similarity of yielding results under the unchanged conditions was calculated for the degree of repeatability and reproducibility. The result is shown in Table 6 (details in Appendix F) and summarized in Fig. 10b. The analysis showed that the % Study Var of PE, PA, and vCF/PA of total %Gage R&R (G) was 9.99%, 23.76% and 25.76%, respectively. G experiment quantified the measurement uncertainty by decomposing total variation into components attributable to the testing system and sample-to-sample differences, as shown in Fig. 10b. The results indicated that most observed variation originated from material heterogeneity (Randomization of specimen forms) rather than instrumental or operator errors. Therefore, the test system demonstrated acceptable repeatability and reproducibility even for hygrothermal-sensitive composites. This analysis directly resolved **Q2** and **Q5** by identifying and quantifying the primary sources of uncertainty, ensuring that the MFI results are statistically reliable and reproducible.

Correspondingly, the intuitive scale: Number of Distinct Categories (NDC) method was conducted by

$$NDC = int\left(\frac{\sqrt[2]{2\left(1-G^2\right)}}{G}\right) \tag{2}$$

The NDC represents the number of non-overlapping confidence intervals, which indicates the acceptance of the measurement system, the minimum threshold value is 5[42]. The analysis suggested that the repeatability and reproducibility of the test system were acceptable because the NDC evaluation of PE, PA, and vCF/PA was 14, 5, and 5, respectively. When NDC ≥ 5, the precision-to-tolerance ratio (P/T ratio) of the test system is less than 10%, which suggests the CI of the system is larger than 99.73% based on the normal distribution of the underlying gauge error[42]. The P/T ratio of PE, PA, and vCF/PA was described by % tolerance of total G, which were 1.49%, 8.49% and 4.59%, respectively. It showed that the test result of PE was excellent (NDC highly the better), whilst it also concludes that the measurement of PA and nylon-based composite significantly lowers the accuracy of test results due to the smaller NDC and larger P/T ratio than the related value of PE. However, considering NDC = 5, the PA and nylon-based composite measurements were marginally acceptable[42]. Alternatively, the variance from measurement arrangements, which is the % contribution of total G, was pretty low compared to part-to-part variation, indicating the high confidence of the measurement, especially when the value of % contribution is below 4%, such as PE[43]. The high reproducibility rate led substantial credence to the MFI measurement due to the non-contribution of variation, as shown in Fig. 10. The distinction of pellet forms caused a relatively significant difference during the test, which was depicted by the % contribution of part-to-part. But fortunately, the value of repeatability was less than 10%, which illustrated the validity and reliability of the experiment. It is reassuring to note that all verification tests according to optimized test conditions, especially the pre-heat time (1

min for vCF/PA), exhibited the good repeatability, less than a critical value of 5% which illustrated the acceptable correct result based on ISO 5725-2[12]. The reproducibility of PA and vCF/PA has been significantly improved compared with the previous RSM experiment, which was conducted without optimized test conditions. Adopting this method, the repeatability and reproducibility of PA were up to 4.873% and 38.248%, respectively, which was better than the previously published result (7.988% and 35.863%, respectively, outliers removed)[15]. At the same time, the repeatability and reproducibility of vCF/PA were close to the test results of benchmark materials, 3.179% and 12.208%, respectively. The reason for the improvement of the accuracy of vCF/PA is a higher nominal test load (5 kg $>$2.16 kg) compared with the test of PA, an increase of melt extrusion speed when the large load was significantly applied reduced the potential risk of thermal degradation, thus, achieved a high precision of the measurement with a relatively short time of extrusion.

Conclusion

This study developed a combined RSM–MSA framework to systematically identify and optimize key parameters influencing the MFI measurement of hygrothermal-sensitive polymer composites. The response surface analysis demonstrated that test load, temperature, and drying time statistically affect MFI values and repeatability significantly. In contrast, pre-heating time primarily affects the repeatability through thermal stabilization and degradation control.

The optimized pre-heat duration predicted by the transient thermal simulation successfully matched the experimental data, confirming the validity of the one-dimensional transient heat conduction model. This optimization improved the repeatability and reproducibility of polyamide-based composites and enhanced the consistency across different testing sessions. Compared with the interlaboratory benchmark study previously[15], our research advances from an empirical precision evaluation to a mechanistically guided optimization and simulation framework, introducing a framework for long-term calibration and transferability. These improvements make the method more physically interpretable and practically applicable for manufacturing hygrothermal-sensitive composites. Taking PA as an example, this study reduced the MFI test repeatability error from about 8.2% reported in the literature to 4.837%, an improvement of roughly 40%; meanwhile, the reproducibility was optimized from approximately 40.7% to around 38.248%. Although the testing system here was more complex (involving carbon fibers and composite materials), the overall fluctuation was even better: repeatability and reproducibility of vCF/PA were up to 3.179% and 12.208%, respectively. This demonstrates that the proposed method in this study outperforms the literature standards regarding controllability, stability, and transferability, providing a more reliable and standardized basis for rheological testing of hygrothermal-sensitive polymers and composite systems.

Importantly, the optimized parameters are directly translatable to industrial extrusion and FDM conditions. The load and thermal histories in the laboratory MFI test were aligned with typical extrusion shear rates, residence times observed in industrial-scale processing and FDM procedures, indicating that the identified parameter window, e.g., drying 6.6 h, preheating 1–3 min, and load up to 5 kg (FDM printing via 0.6 mm nozzle, for details see Appendix C) can serve as a reference for quality control and process design in actual filament fabrication and printing environments.

Overall, this research bridges the gap between laboratory-scale MFI testing and real manufacturing conditions, contributing to the establishment of a credible, reproducible, and application-oriented rheological characterization method for moisture- and temperature-sensitive composite materials.

Data availability

To request the experimental information and data presented in this study, please contact the corresponding author.

Received: 24 September 2025; Accepted: 23 December 2025
Published online: 24 January 2026

References

1. Shenoy, A. *Thermoplastic Melt Rheology and Processing* (CRC, 1996).
2. Wang, S., Capoen, L., D'hooge, D. R. & Cardon, L. Can the melt flow index be used to predict the success of fused deposition modelling of commercial poly(lactic acid) filaments into 3D printed materials? *Plast., Rubber Compos.* **47**, 9–16. https://doi.org/10.1080/14658011.2017.1397308 (2018).
3. Fujiyama, M. Structure and properties of injection moldings of β-crystal Nucleator-Added polypropylene: part 2 effect of MFI of base resin. *Int. Polym. Proc.* **10**, 251–254 (1995).
4. Sikora, J. & Dulebová, L. *Technological and Dessign Aspects of the Processing of Composites and nanocomposites, Vol. II* (Politechnika Lubelska, Lublin University of Technology Publishing House,, 2019).
5. Tian, X., Liu, T., Yang, C., Wang, Q. & Li, D. Interface and performance of 3D printed continuous carbon fiber reinforced PLA composites. *Compos. Part A: Appl. Sci. Manufac.* **88**, 198–205. https://doi.org/10.1016/j.compositesa.2016.05.032 (2016).
6. Boparai, K. S., Singh, R. & Singh, H. Process optimization of single screw extruder for development of nylon 6-Al-Al2O3 alternative FDM filament. *Rapid Prototyp. J.* **22**, 766–776. https://doi.org/10.1108/rpj-09-2014-0119 (2016).
7. Singh, R., Singh, S. & Fraternali, F. Development of in-house composite wire based feed stock filaments of fused deposition modelling for wear-resistant materials and structures. *Compos. Part. B: Eng.* **98**, 244–249. https://doi.org/10.1016/j.compositesb.2016.05.038 (2016).
8. Singh, R., Bedi, P., Fraternali, F. & Ahuja, I. P. S. Effect of single particle size, double particle size and triple particle size Al2O3 in Nylon-6 matrix on mechanical properties of feed stock filament for FDM. *Compos. Part. B: Eng.* **106**, 20–27. https://doi.org/10.1016/j.compositesb.2016.08.039 (2016).
9. Bedi, P., Singh, R. & Ahuja, I. P. S. Effect of SiC/Al2O3 particle size reinforcement in recycled LDPE matrix on mechanical properties of FDM feed stock filament. *Virtual Phys. Prototyp.* **13**, 246–254. https://doi.org/10.1080/17452759.2018.1496605 (2018).

10. Sa'ude, N., Ibrahim, M. & Ibrahim, M. H. I. Mechanical properties of highly filled iron-ABS composites in injection molding for FDM wire filament. *Materials Sci. Forum* **773–774**, 448–453 (Trans Tech Publ). https://doi.org/10.4028/www.scientific.net/MSF (2014).
11. Agarwala, M. et al. in *1996 International Solid Freeform Fabrication Symposium*.
12. Rides, M. & Allen, C. The use of the melt flow rate method for moisture sensitive materials and an evaluation of the uncertainties in melt flow rate measurement. NPL Report. MAT 3 (2007).
13. Shida, R. & Cancio, L. Correlation of low density polyethylene rheological measurements, with optical and processing properties. *Polym. Eng. Sci.* **17**, 769–774 (1977).
14. Smith, D. J. The correlation of melt & index and extrusion coating resin performance. *Physicochem. Polym.*, Tappi, **60**, (1977).
15. Rides, M., Allen, C., Omloo, H., Nakayama, K. & Cancelli, G. Interlaboratory comparison of melt flow rate testing of moisture sensitive plastics. *Polym. Test.* **28**, 572–591. https://doi.org/10.1016/j.polymertesting.2009.03.013 (2009).
16. Shenoy, A. & Saini, D. Melt flow index: more than just a quality control rheological parameter. Part I. *Adv. Polym. Technol.* **6**, 1–58 (1986).
17. Guerreiro, S. D. C., João, I. M. & Pimentel Real, L. E. Evaluation of the influence of testing parameters on the melt flow index of thermoplastics. *Polym. Test.* **31**, 1026–1030. https://doi.org/10.1016/j.polymertesting.2012.07.008 (2012).
18. Kim, S. S. & Han, C. D. Effect of thermal history on the rheological behavior of a thermotropic liquid-crystalline polymer. *Macromolecules* **26**, 3176–3186 (1993).
19. Myers, R. H. a. *Response surface methodology: process and product optimization using designed experiments / Raymond H. Myers, Douglas C. Montgomery, Christine M. Anderson-Cook*. Fourth edition. edn, (2016).
20. Box, G. E., Hunter, J. S. & Hunter, W. G. *Statistics for Experimenters: design, innovation, and Discovery* (Wiley, 2005).
21. Krassig, H. A. *Fiber Technology: from Film To Fiber* Vol. 4 (CRC, 1984).
22. Garg, H. Investigations for melt flow index of Nylon6-Fe composite based hybrid FDM filament. *Rapid Prototyp. J.* **22**, 338–343. https://doi.org/10.1108/RPJ-04-2014-0056 (2016).
23. Giles, H. F. Jr, Mount, I. I. I., Wagner & Jr E. M. J. R. *Extrusion: the definitive processing guide and handbook*. William Andrew. (2004).
24. Lanzotti, A., Grasso, M., Staiano, G. & Martorelli, M. The impact of process parameters on mechanical properties of parts fabricated in PLA with an open-source 3-D printer.*Rapid Prototyping J.*. **21** 604–617. https://doi.org/10.1108/rpj-09-2014-0135 (2015).
25. Van Krevelen, D. W. & Te Nijenhuis, K. in *Properties of Polymers (Fourth Edition)* (eds D. W. Van Krevelen & K. Te Nijenhuis) 799–818 (Elsevier, 2009).
26. Seeger, A., Freitag, D., Freidel, F. & Luft, G. Melting point of polymers under high pressure: part II. Influence of gases. *Thermochim. Acta*. **486**, 46–51. https://doi.org/10.1016/j.tca.2008.12.023 (2009).
27. Poletto, M. Influence of coupling agents on rheological, thermal expansion and morphological properties of recycled Poypropylene wood flour composites. *Maderas Ciencia Y tecnología*. **20**, 563–570 (2018).
28. Ramanath, H. S., Chua, C. K., Leong, K. F. & Shah, K. D. Melt flow behaviour of poly-ε-caprolactone in fused deposition modelling. *J. Mater. Science: Mater. Med.* **19**, 2541–2550. https://doi.org/10.1007/s10856-007-3203-6 (2008).
29. Mostafa, N., Syed, H. M., Igor, S. & Andrew, G. A. Study of melt flow analysis of an ABS-Iron composite in fused deposition modelling process. *Tsinghua Sci. Technol.* **14**, 29–37. https://doi.org/10.1016/S1007-0214(09)70063-X (2009).
30. Kuznetsov, V. E., Solonin, A. N., Tavitov, A. G., Urzhumtsev, O. D. & Vakulik, A. H. Increasing of strength of FDM (FFF) 3D printed parts by influencing on temperature-related parameters of the process. *Rapid Prototyp. J.* 1–32. https://doi.org/10.20944/preprints201803.0102.v2 (2018).
31. Kim, J. optimization of design and manufacturing process of fusion filament fabrication (FFF) 3D printing. Ph.D. Thesis, West Virginia University, Morgantown, WV, USA (2018).
32. Sa'ude, N., Ibrahim, M. & Ibrahim, M. Melt flow rate (MFR) of abs-copper composite filament by fused deposition modeling (FDM). *ARPN J. Eng. Appl. Sci.* **11**, 6562–6567 (2016).
33. Mackay, M. E. The importance of rheological behavior in the additive manufacturing technique material extrusion. *J. Rheol.* **62**, 1549–1561. https://doi.org/10.1122/1.5037687 (2018).
34. Peruchi, R. S., Balestrassi, P. P., de Paiva, A. P. & Ferreira, J. R. Santana Carmelossi, M. A new multivariate Gage R&R method for correlated characteristics. *Int. J. Prod. Econ.* **144**, 301–315. https://doi.org/10.1016/j.ijpe.2013.02.018 (2013). de.
35. Runje, B., Novak, A. H. & Razumić, A. in *XVII International Scientific Conference on Industrial Systems*. 274–277 (2017).
36. Montgomery, D. C. Design and Analysis of Experiments, 9th Edition. *Wiley.com* (2017).
37. Becker, M. in *Heat Transfer: A Modern Approach* (ed Martin Becker) 85–116 Springer US, (1986).
38. Daneshpayeh, S., Ashenai Ghasemi, F., Ghasemi, I. & Ayaz, M. Predicting of mechanical properties of PP/LLDPE/TiO2 nano-composites by response surface methodology. *Compos. Part. B: Eng.* **84**, 109–120. https://doi.org/10.1016/j.compositesb.2015.08.075 (2016).
39. Molugaram, K. & Rao, G. S. in *Statistical Techniques for Transportation Engineering* (eds Kumar Molugaram & G. Shanker Rao) 451–462 (Butterworth-Heinemann, 2017).
40. Mee, R. W. & Xiao, J. Steepest ascent for Multiple-Response applications. *Technometrics* **50**, 371–382. https://doi.org/10.1198/004017008000000271 (2008).
41. Cengel, Y. & Ghajar, A. Transient heat conduction. *Heat mass. Transfer: Fundamentals Applications*, McGraw-Hill Education: New York, NY, USA, 228 (2011).
42. Pan, J. N., Li, C. I. & Ou, S. C. Determining the optimal allocation of parameters for multivariate measurement system analysis. *Expert Syst. Appl.* **42**, 7036–7045. https://doi.org/10.1016/j.eswa.2015.04.038 (2015).
43. Kaija, K. et al. Inkjetting dielectric layer for electronic applications. *Microelectron. Eng.* **87**, 1984–1991 (2010).

Acknowledgements

The authors would like to acknowledge the support of the General Program of Education of Zhejiang Province (No. Y202456090) and the financial support from Ningbo S&T Bureau under the 2024 Commonweal Research Program (Project code: 2024S068).

Author contributions

**Ning Su: ** Conceptualization, Methodology, Data curation, Visualization, Writing – original draft, **Xiaoling Liu: ** Conceptualization, Methodology, Writing – review & editing, **Xiang Chen & Jiafei Gu: ** Conceptualization, Writing – review & editing, **Jing Bai: ** Conceptualization, Supervision, Methodology, Writing – review & editing.

Funding

This research has received funding from the Ningbo Municipal Bureau of Science and Technology, under the 2024 Commonweal Research Program (Project code: 2024S068).

Declarations

Competing interests
The authors declare no competing interests.

Additional information
Supplementary Information The online version contains supplementary material available at https://doi.org/10.1038/s41598-025-33933-4.

Correspondence and requests for materials should be addressed to J.B.

Reprints and permissions information is available at www.nature.com/reprints.

Publisher's note Springer Nature remains neutral with regard to jurisdictional claims in published maps and institutional affiliations.